

Seismic behavior of steel eccentrically braced frames under soft-soil seismic sequences

Jorge Ruiz-García^{a,*}, Edén Bojorquez^b, Edgar Corona^b

^a Facultad de Ingeniería Civil, Universidad Michoacana de San Nicolás de Hidalgo, Edificio C, Planta Baja, Cd. Universitaria, 58040 Morelia, Mexico

^b Facultad de Ingeniería Civil, Universidad Autónoma de Sinaloa, Calz. de las Américas y Boulevard Universitarios, Cd. Universitaria, 80040 Culiacán, Mexico

ARTICLE INFO

Keywords:

Eccentrically braced frame
Soft soils
Link rotation
Seismic sequences
Aftershocks

ABSTRACT

The goal of this paper is to examine the seismic response of eccentrically braced frames (EBFs) under artificial narrow-band mainshock-aftershock sequences by means of detailed analytical models representative of buildings designed under the Mexico City Code criteria. These analytical models take into account the nonlinear behavior of the links including a failure criterion. Relevant results for engineering practice showed that strong aftershocks could significantly increase interstory drift demands once the link fails, while surrounding members (adjacent beams, columns) behave nonlinearly, which is opposite to the design philosophy. In addition, it was noted the nonuniform distribution of hysteretic energy along-height of the links, which do not take fully advantage of the energy dissipating capacity of the shear links.

1. Introduction

Eccentrically Braced Frames (EBF) have become an attractive earthquake-resistant structural system in many countries worldwide since it provides high levels of both elastic stiffness (similar to concentrically braced frames) and ductility (similar to moment-resisting frames). In EBFs, the seismic energy induced to the building during earthquake loading is dissipated through the inelastic behavior of the links, while the remaining elements (beams, columns, and braces) are expected to behave elastically. Currently, the design procedure for EBF is prescribed in the 2016 AISC Seismic Provisions for Structural Steel Buildings [1], which specifies the link design, link rotation limits, and link overstrength factors, among other issues. Particularly, the link rotation is limited to 0.08 rad for links behaving in shear (i.e. for links with length equal or smaller than $1.6M_p/V_p$, where M_p and V_p are the plastic bending moment and the plastic shear strength of the link). A comprehensive review of relevant experimental and analytical research carried out on steel eccentrically braced frames is presented in Ref. [2].

The first reported worldwide failure in EBFs was observed in St. Asaph Street parking structure in the city of Christchurch as a consequence of the February 22, 2011 ($M_w = 6.3$) earthquake that struck the Canterbury region in New Zealand. A detailed forensic examination revealed that three main factors led to the unsatisfactory performance of this structure [3,4]: a) the intensity of the ground shaking (several times the intensity that was expected during a design-level event), b)

the frame geometry, which severely amplified the imposed seismic demands, and c) observed fracture in the links from an erection (fit-up) error, since the link stiffener was not located (as specified) directly above the brace flange, producing a severe strain concentration. Although not examined in the aforementioned study, it should be noted that the February 22, 2011 seismic event was part of a sequence of strong earthquakes that hit the New Zealand's South Island that began with the September 3, 2010 ($M_w = 7.0$) Canterbury earthquake. Therefore, this lesson motivates examination of the behavior of EBFs in seismic regions under strong earthquakes (mainshock) and, in general, under seismic sequences.

It should be noted that it has been a growing interest in incorporating EBFs as a lateral-load resisting system for new buildings in Mexico City, as shown in Fig. 1. However, until recently, the Technical Requirements for Design of Steel Structures released in the 2017 Mexico City Construction Code [5] included design specifications for eccentric braced frames for the first time, which are entirely based on Ref. [1]. In addition, the 2017 Mexico City Construction Code prescribe a limiting maximum interstory drift of 0.02 to avoid collapse for the design of EBFs. However, there is a lack of information about the performance of EBFs built on very soft soil sites to judge at what levels of seismic intensity the EBFs can reach or exceed this limiting drift.

For the case of Mexico City, Mexican practicing engineers know that buildings, and other civil engineering structures, built on the former bed-lake of Mexico City are exposed to narrow-band earthquake ground

* Corresponding author.

E-mail address: jruizgar@stanfordalumni.org (J. Ruiz-García).



Fig. 1. Examples of the use of eccentric braced frames in buildings: a) short link, b) long link.

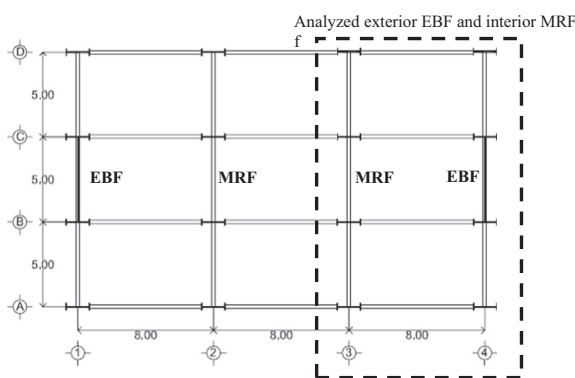


Fig. 2. Plan view of case-study steel buildings [units in meters].

motions characterized by relatively long predominant periods and low-frequency content, along with large energy demands e.g., [6–8]. In addition of this fact, buildings might also be subjected to strong aftershocks that may compromise their structural safety. For instance, a clear example of the effect of strong aftershocks was observed after the September 19, 1985 Michoacan earthquake ($M_w = 8.0$) and the following aftershock on September 20 ($M_w = 7.6$) that struck Mexico City [9]. After these events, it is well documented that medium-rise buildings located in the old bed-lake zone of Mexico City suffered moderate-to-severe structural damage as a consequence of the mainshock and many buildings increased their post-mainshock state of damage, or suffered excessive permanent displacements as a result of the strong aftershock that shook the city the following day [9]. In spite of the 1985 experience, very limited research has been conducted to investigate the effect of aftershocks in the response of buildings located in soft soil sites, in such a manner as to caution practicing engineers about the importance of considering full seismic sequences during earthquake-resistant design, and the few studies focused on building moment-resisting frames [10,11] and buckling-restrained braced frames [12] as structural system for buildings. Therefore, evaluating the seismic behavior of buildings incorporating EBFs under a strong mainshock and aftershock ground motions is pertinent and relevant for the Mexican structural engineering community.

The primary objective of the research reported in this paper was to investigate the seismic behavior of eccentrically braced frames (EBFs) subjected to both mainshock earthquake ground motions and mainshock-aftershock earthquake ground motions sequences representative of those recorded in the soft-soil sites of Mexico City. For this purpose, two typical steel office buildings having 4- and 8-story incorporating EBFs were designed as part of this investigation. The case-study

buildings were modeled and analyzed with the computational platform *OpenSees* [13]. Particular emphasis was placed in the nonlinear modeling of the links, which includes a failure criterion. It should be mentioned that the particular influence of the soil-structure interaction in the seismic response of the case-study building models was outside of the scope of the paper.

2. Case-study EBF buildings

2.1. Description and design of EBFs

Two steel buildings having 4 and 8 stories were considered as part of this investigation. The buildings were assumed to be designed for office occupancy and located in the lake-bed zone of Mexico City. They were designed by an experienced structural engineering office to satisfy the 2004 Edition of the Technical Requirements for Seismic Design included in the Mexico City Building Construction Code [14]. Fig. 2 shows the typical plan view of the steel buildings. Moment-resisting frames (MRF) were provided in the longitudinal direction, while exterior EBFs and interior MRF acting as a dual system were incorporated in the transverse direction. Design of interior frames as MRFs is a common assumption in Mexican structural engineering practice. The EBFs were incorporated for drift control since the weak-axis of the columns is oriented in this direction as shown in Fig. 2. Therefore, the lateral stiffness is similar in both directions to avoid torsional effects during the seismic response. Fig. 3 displays the distribution along height of the frames including position of eccentric braces. A typical story height of 3.5 m was assumed for both buildings. Design dead load of 680 kgf/cm^2 (66.69 MPa) were assumed for all stories, while design live load of 70 kgf/cm^2 (6.86 MPa) and 180 kgf/cm^2 (17.65 MPa) for the roof and typical story, respectively, were considered according to the Mexico City Building Construction Code. An equivalent static linear analysis, which is commonly used in the Mexican design practice, assuming a triangle inverted distribution of code-specified base shear was employed for sizing the frame members. For this purpose, elastic acceleration design spectrum ordinates were reduced by a response modification factor equal to 3 and 4 in the longitudinal and transverse direction, respectively, which takes into account the ability of the structure to undergo inelastic deformations, without consideration of structural overstrength. Particularly, links in the EBFs were set as 1.0 m long to design short links expected to fail in shear. It was also assumed a plastic rotation capacity of 0.06 rad and an overstrength factor equal to 1.5 to compute the shear web capacity in the links. Square HSS steel sections were employed as diagonal braces assuming a nominal yield strength of 3515 kgf/cm^2 (344.7 MPa). Tables 1, 2 reports the final sections of the links and braces for the 4- and 8-story frames,

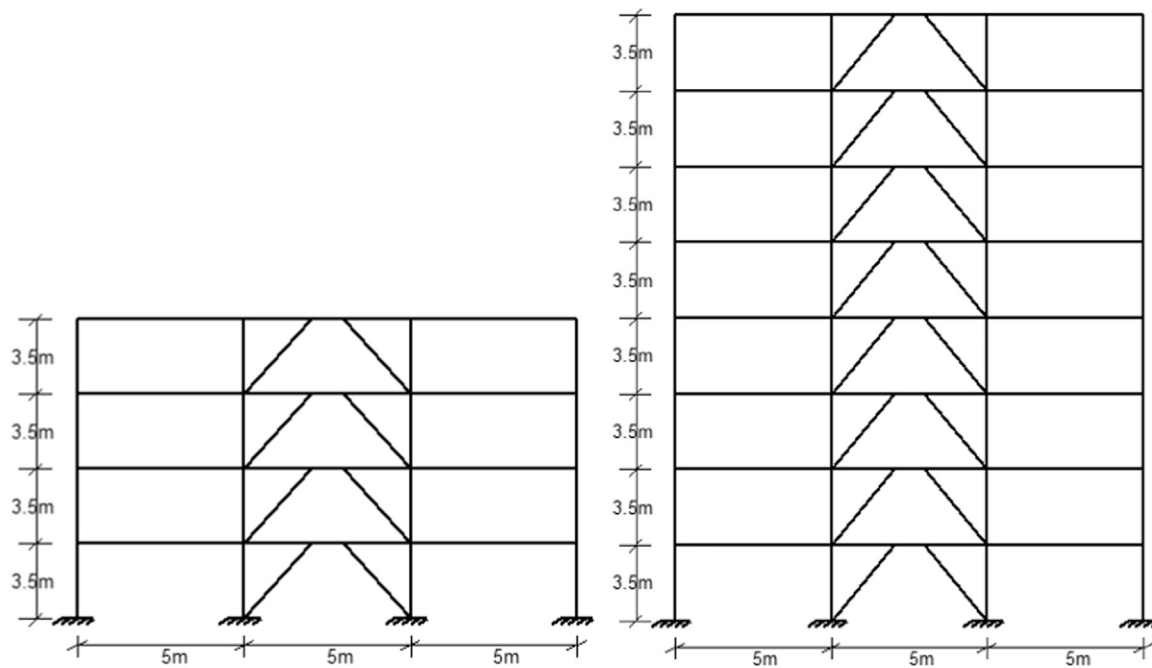


Fig. 3. Geometry of the case-study steel office buildings.

Table 1
Steel sections for the links and braces of the 4-story frame.

Story	Links	Braces
4	W16 × 40	HSS 8 × 8 × 5/16"
3	W16 × 45	HSS 8 × 8 × 5/16"
2	W16 × 57	HSS 8 × 8 × 5/16"
1	W16 × 67	HSS 8 × 8 × 5/16"

Table 2
Steel sections for the links and braces of the 8-story frame.

Story	Links	Braces
8	W18 × 50	HSS 8 × 8 × 5/16"
7	W18 × 50	HSS 8 × 8 × 5/16"
6	W 18 × 60	HSS 8 × 8 × 5/16"
5	W 18 × 65	HSS 8 × 8 × 5/16"
4	W 18 × 71	HSS 8 × 8 × 5/16"
3	W 18 × 71	HSS 8 × 8 × 5/16"
2	W 21 × 83	HSS 8 × 8 × 3/8"
1	W 21 × 83	HSS 8 × 8 × 3/8"

respectively. Detailed information about the design process of the case-study buildings is available in Refs. [36,37].

2.2. Modeling of the case-study EBFs

The case-study buildings were modeled using the computational platform *OpenSees* [13]. Only half of the buildings were modeled due to their symmetry in the building's plan. Two-dimensional (2D) centerline analytical models that included one exterior EBF and one interior MRF in parallel were prepared for each building as noted in Fig. 2. Columns were assumed fixed at their base. Beams, columns, and braces were modeled using a distributed plasticity approach, which included fiber-based steel cross sections with nine integration points along each member. The Giuffrè-Menegotto-Pinto (steel02 material in the *OpenSees* library [13]), which allow simulating kinematic strain hardening and the *Bauschinger* effect, was selected for modeling the steel nonlinear behavior. It should be noted that the Giuffrè-Menegotto-Pinto material model does not allow stiffness and strength degradation, but it is

expected that beams, columns, and braces mainly behave in an elastic manner that preclude exhibiting local buckling under seismic loading following the design philosophy for eccentric braced frames. It should also be noted that the slab contribution was not taken into account in the beams.

Additionally, panel zone flexibility was taken into account in each building model following the modeling technique proposed in [15]. The panel zone was modeled as a four-element hinged parallelogram with a nonlinear rotational spring to represent its shear nonlinear hysteretic behavior, which is assumed to include a tri-linear backbone without stiffness and strength deterioration as proposed by Krawinkler [16].

2.3. Modeling of links

For the purpose of modeling the nonlinear behavior of the links, several approaches have been proposed in the literature e.g. [2,17,19,25–28]. The introduced analytical models aim to capture the particular hysteretic features (e.g. kinematic and/or isotropic hardening, *Bauschinger* effect) in the shear force-link rotation angle and the bending moment-link rotation angle in the cyclic response showed during experimental tests. In general, the simulation response provided by the analytical models can be classified as piecewise e.g. [17,19,25,26] and smooth e.g. [27]. An interesting comparison of the ability of four analytical models to capture the experimental cyclic response of short, intermediate, and long links is presented by Bosco et al. [27]. The authors highlighted that a better accuracy in the hysteretic response simulation for the three types of links is found for the analytical model providing a smooth response than those providing a piecewise response. For this study, the shear link modeling strategy suggested by Prinz [18] for implementation in *OpenSees* [13], which is based on the approach introduced by Richards [17], was taken into account in this investigation. According to Bosco et al. [27], the analytical model introduced by Richards [17] which is a modified version of the analytical model proposed by Ramadan and Ghobarah [19], still provides a good prediction of the cyclic response of short links. In this modeling approach, the shear links are composed by an elastic beam element with three translational springs at either end acting in parallel, as illustrated in Fig. 4a. For this purpose, two nodes at each end of the link, referred to as the external and internal nodes, were defined to have

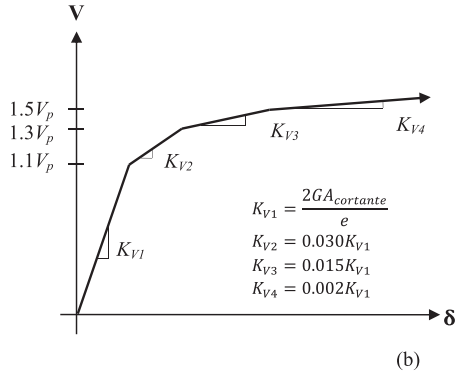
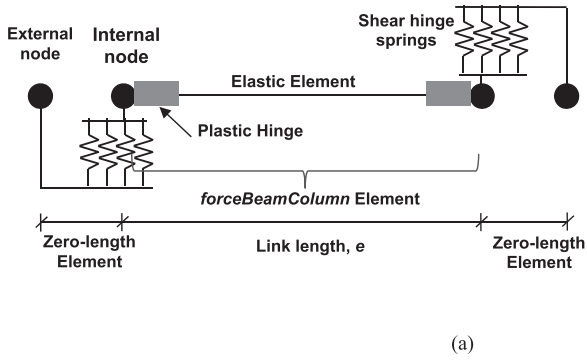


Fig. 4. a) Schematic representation of the link model, b) combined force-deformation relationship for translational springs at each end.

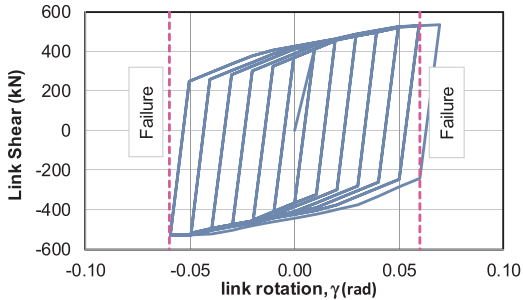


Fig. 5. Analytical hysteretic response of short links considered in this study based on the modeling approach described in Ref. [18].

the same coordinates (i.e. zero-length spring element). Each translational spring has a bilinear force-deformation behavior, and they act in parallel to lead a multi-linear force-deformation envelope, as shown in Fig. 4b, that simulate a shear plastic hinge. Following this modeling strategy, it was assumed that the shear links exhibits the hysteretic behavior showed in Fig. 5.

Under the aforementioned modeling assumptions, the 4-story, denoted as 4N_EBF, and the 8-story frames, 8N_EBF, have fundamental

Table 3

List of earthquake ground motions employed to derive the artificial seismic sequences considered in this investigation.

Date	Ms	Station Name	Station ID [23]	Comp.	PGA (cm/s ²)	PGV (cm/s)	T _g (s)	t _D (s)
M1	25/04/1989	Villa del mar	29	EW	46.5	15.3	2.96	95.8
M2	25/04/1989	Villa del mar	29	NS	49.4	22.0	2.96	82.0
M3	25/04/1989	Jamaica	43	NS	35.2	15.6	3.04	73.7
M4	25/04/1989	Rodolfo Menéndez	48	EW	47.7	18.8	2.89	73.4
R5	25/04/1989	P.C.C. Superficie	25	EW	42.5	15.4	2.32	61.5
R6	14/04/1989	Córdoba	56	EW	45.2	11.2	2.33	70.2
R7	25/04/1989	Liverpool	58	EW	40.0	12.4	2.29	75.5
R8	14/04/1989	Roma-B	RB	EW	23.6	4.8	2.30	89.1

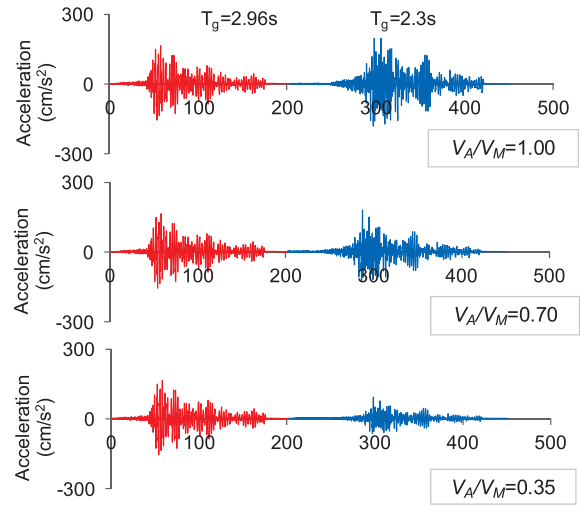


Fig. 6. Examples of artificial seismic sequences considered in this study for three different V_A/V_M ratios.

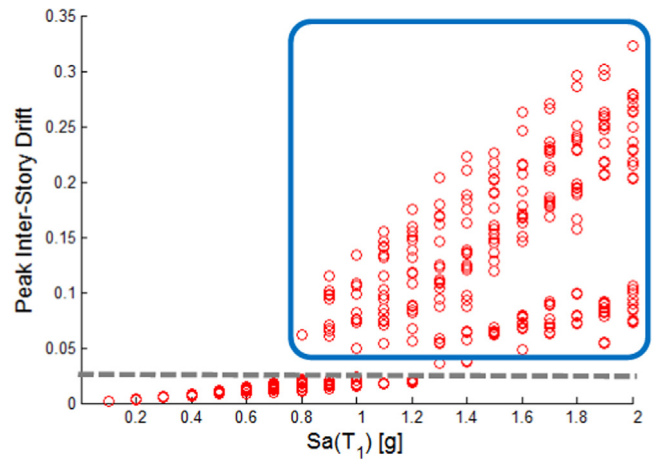


Fig. 7. IDA of model 4N_EBF subjected to the seismic sequences with $V_A/V_M = 1$.

periods of vibration of 0.77 s and 1.32 s, respectively.

2.4. Failure criterion for shear links

The AISC 341-16 [1] specifications indicates that the inelastic link rotation, γ_p (i.e. the link rotation after removing the elastic rotation from the link rotation, γ) for short links should not exceed 0.08 rad. However, experimental evidence (e.g. Okazaki and Engelhardt [20] and Okazaki et al. [21]) has revealed that links can fail at plastic link rotation smaller than 0.08 rad. For instance, Specimen 4 A (link specimen

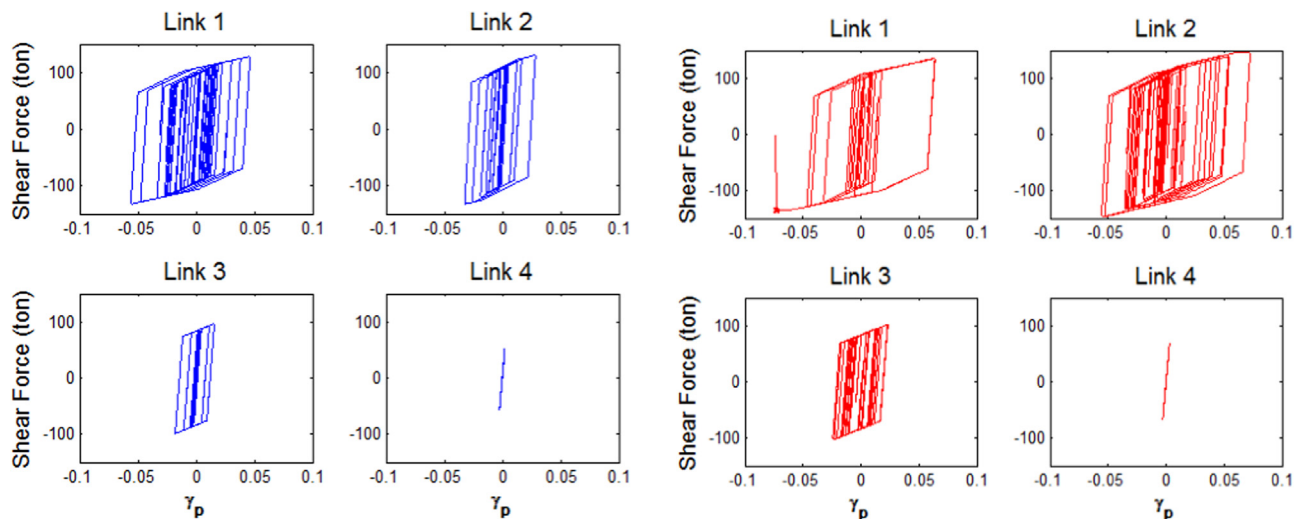


Fig. 8. Hysteretic response of the links in model 4N_EBF subjected to the sequence M2M3 ($V_A/V_M = 1$) for an intensity of 0.8 g: a) considering mainshock, and b) during the mainshock-aftershock sequence. (For interpretation of the references to color in this figure legend, the reader is referred to the web version of this article.)

was made of a W10x33 section with ASTM A992 steel) exhibited link web fracture that led to sudden strength degradation and premature link failure [20]. It was also reported that the link web fracture limited the plastic rotation capacity of 0.06 rad. On the other hand, Gulec et al. [22] assembled a database of experimental results from 110 EBF link specimens tested under monotonic loading and 107 specimens tested under reversed cyclic loading to develop fragility curves for EBF links. Fragility curves that represent the exceedance probability of reaching or exceeding a method of repair for EBF links (e.g. cosmetic, concrete replacement, heat straightening, and link replacement) conditioned on the plastic link rotation were developed in their work. From their statistical analyses, the authors identified that links that suffered minor web and flange local buckling which can be repaired using heat straightening experienced a median plastic link rotation of 0.06 rad. Major damage such as lateral torsional buckling, web fracture, and flange fracture was related to median plastic link rotation of 0.079 rad. Based on the aforementioned observations from Gulec et al. [22], it was decided to incorporate a failure criterion in the analytical model. That is, if the link reaches a plastic link rotation of 0.06 rad in a hysteretic cycle under earthquake ground motion excitation, then the link shear is unable of carrying additional load capacity in the subsequent cycle. However, it should be recognized that the sudden loss of strength and stiffness shown in the experimental response (e.g., in Specimen 4A [20]) is not captured in the analytical hysteretic response as shown in Fig. 5.

3. Seismic sequences

Prior studies have noted that recorded seismic sequences gathered in the soft soils of Mexico City are scarce and artificial seismic sequences should be employed for evaluating the seismic response of building structures [10–12]. Therefore, for generating artificial seismic sequences, the randomized approach was employed in this study, which consists on ensemble a set of recorded (i.e. real) mainshocks acceleration-time histories, and generating artificial mainshock-aftershock sequences by: 1) selecting a mainshock, and 2) simulating the aftershocks by using the remaining mainshock waveforms in the set, at reduced or identical amplitude with no change in spectral content, as artificial aftershocks e.g. [10–12,29,30]. Following this approach, a set of 8 acceleration time histories gathered at recording stations located on soft soil sites of Mexico City were selected from the Mexican Strong Motion Dataset [23], which are listed in Table 3. In this study, the predominant period of the ground motion, T_g [31] and the significant strong motion

duration [32], t_D , were employed as measures of the frequency content and strong motion duration of the EQGM, respectively. It should be noted that four earthquake records have predominant period of the ground motion, T_g , values around 3.0 s, while the other four have T_g values close to 2.3 s. However, only the earthquake records having T_g around 3.0 s were employed as mainshock ground motions (as noted with the letter M), which mean that the dominant period of the mainshock is close or longer than that of the aftershock. Therefore, both T_g and t_D are consistent with ground motions features that have been observed from real sequences gathered at soft soil sites [10]. For simulating strong mainshocks, each earthquake record employed as mainshock was scaled to reach the peak ground velocity (PGV) registered of the well-known East-West component of the *Secretaría de Comunicaciones y Transportes* (SCT) station during the September 19, 1985 earthquake ($PGV = 61.1$ cm/s). In addition, the 8 earthquake records were scaled, in amplitude, to reach 35%, 70% and 100% of the PGV of the mainshock ground motions when employed as aftershock earthquake ground motions. Therefore, 28 artificial sequences were generated randomly for each V_A/V_M ratio (i.e., 0.35, 0.70, and 1.0, where V_A and V_M are the PGV of the aftershock and the mainshock, respectively) since no repetition of the mainshock waveform was allowed in the set. Fig. 6 shows typical artificial seismic sequences with their three levels of V_A/V_M ratio. It should be noted that for performing nonlinear dynamic analyses, there is a time-gap of 40 s having zero acceleration ordinates between the as-recorded mainshock and the artificial aftershock acceleration time-history to ensure that the systems reach its rest position after free-vibration. Similarly, duration of the aftershock acceleration time-history included zero acceleration ordinates at the end of the excitation.

4. Results

The seismic behavior of the case-study EBFs was investigated through incremental dynamic analysis (IDA) under the set of seismic sequences described in the preceding section. For this purpose, the spectral acceleration corresponding to the first-mode of vibration, $S_a(T_1)$, was chosen as the intensity measure. In this study, interstorey drift (i.e. peak transient lateral displacement normalized with respect to the story height) and the peak interstorey drift, IDR (i.e. maximum interstorey drift all over the stories) were considered as the main engineering demand parameters of seismic demand. For the sake of comparison, the limiting IDR equal to 0.02 prescribed in the Mexico City Construction Code during the design phase for avoiding collapse

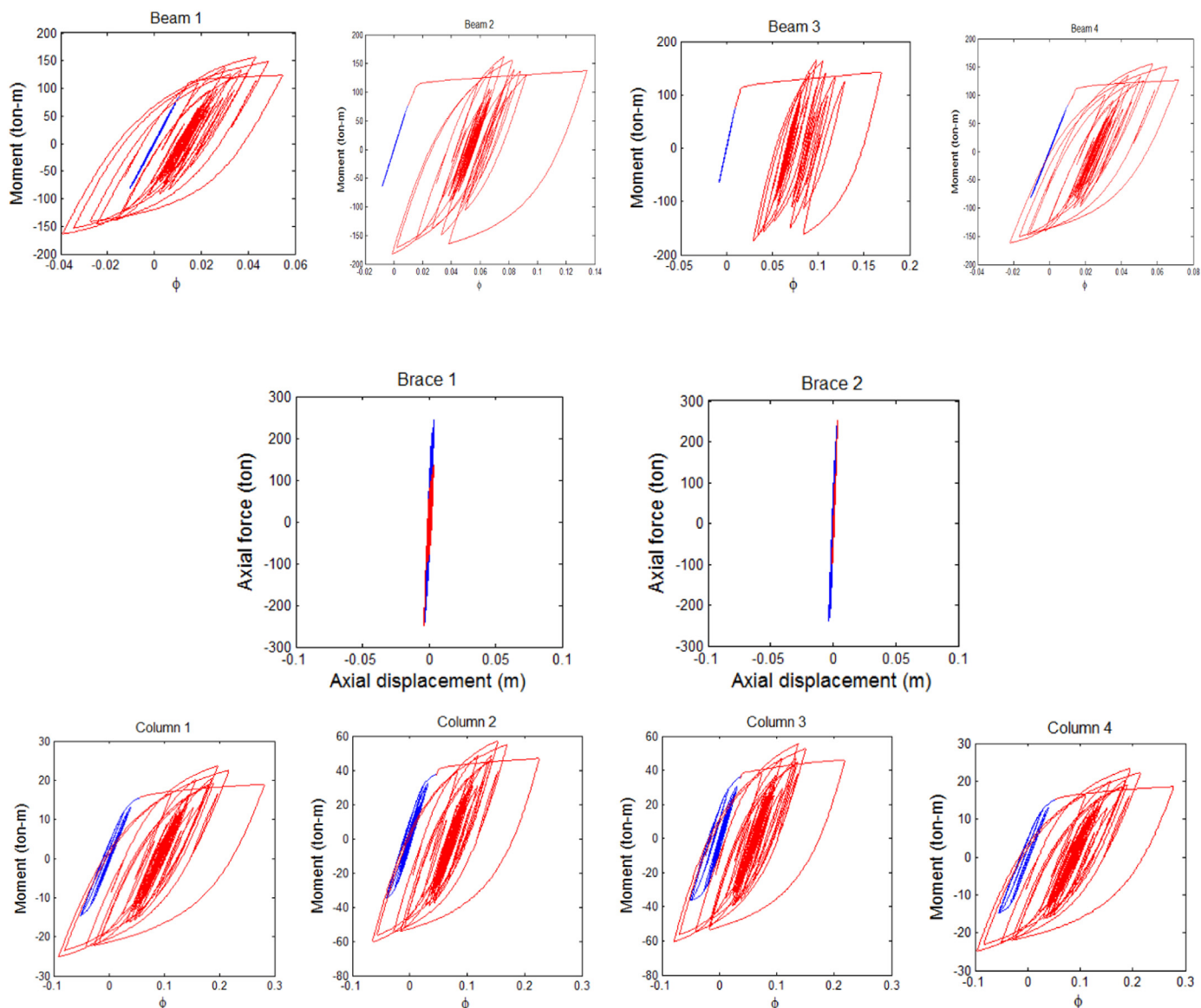


Fig. 9. Hysteretic response of the elements that surround Link 1 (in blue color, the element behavior before the link reaches the failure criterion, and in red color after it reaches the failure criterion). (For interpretation of the references to color in this figure legend, the reader is referred to the web version of this article.)

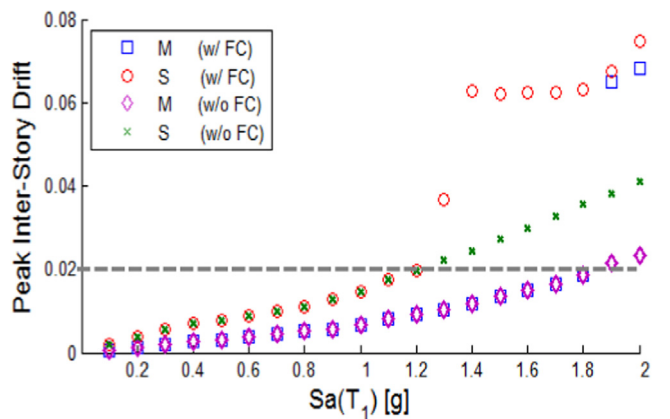


Fig. 10. IDA of model 4N_EBF subjected to the seismic sequences with $V_A/V_M = 1$.

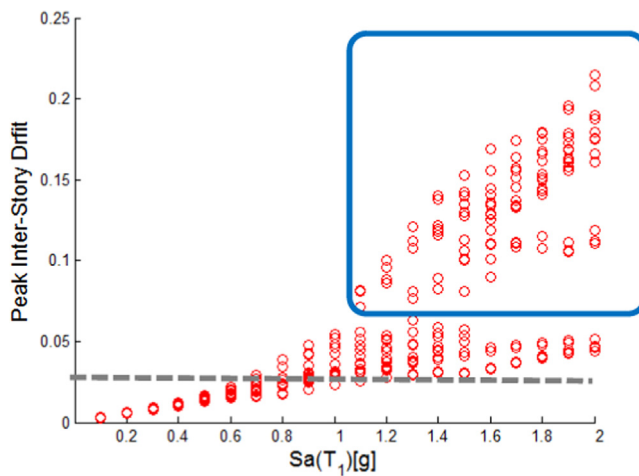


Fig. 11. IDA of model 8N_EBF subjected to the seismic sequences of Set A. (For interpretation of the references to color in this figure, the reader is referred to the web version of this article.)

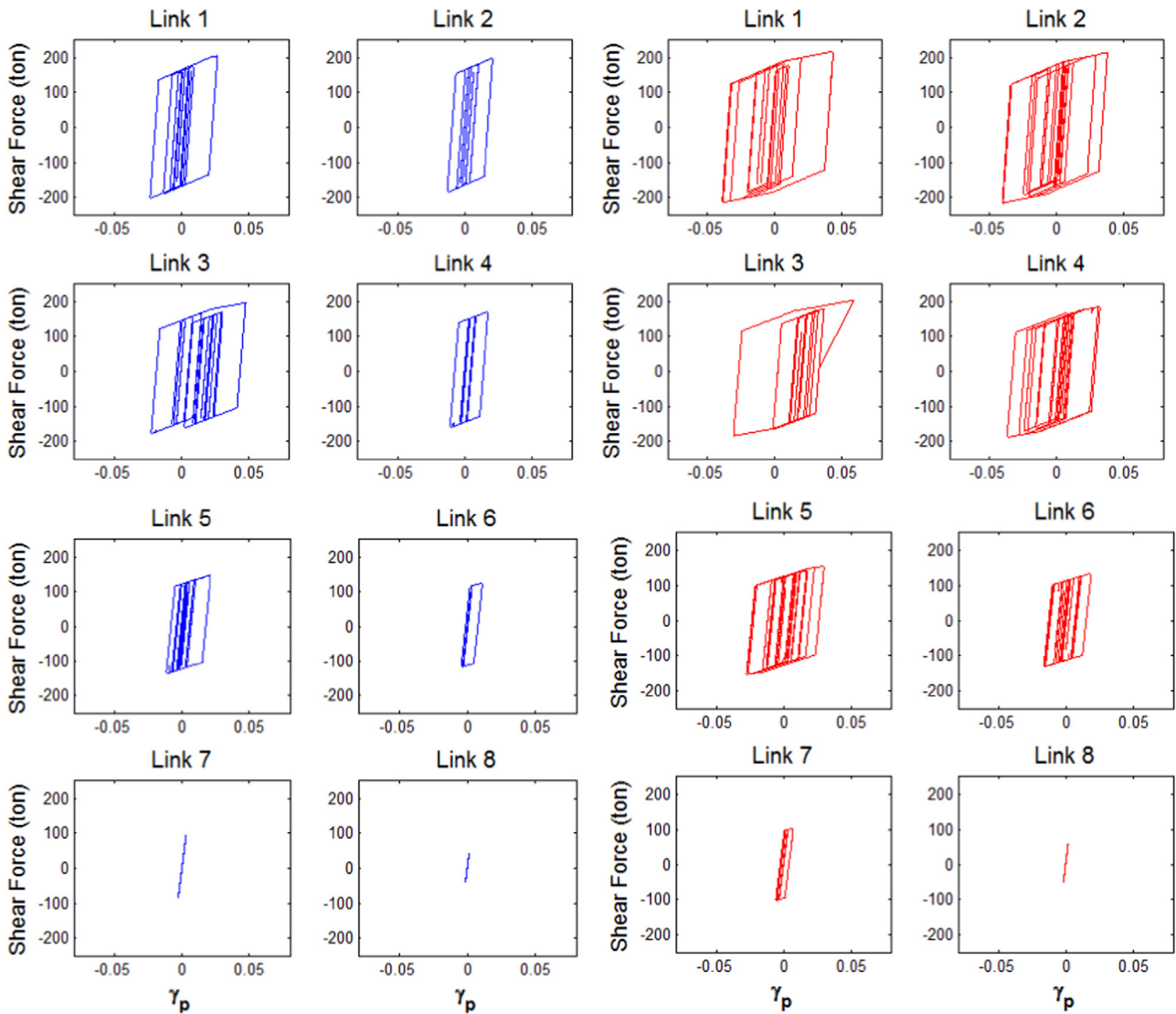


Fig. 12. Hysteretic response of the links of the model 8N_EBF subjected to the sequence M1R5 ($V_A/V_M = 1.0$) for an intensity of 1 g: a) considering mainshock, and b) during the aftershock.

was indicated in grey dashed line.

4.1. Behavior under seismic sequences

Fig. 7 shows the evolution of peak IDR as the ground motion intensity increases of the model 4N_EBF under mainshock-aftershock sequences with $V_A/V_M = 1$. It can clearly be seen that peak IDR significantly increases after an intensity of around $S_a(T_1) = 0.8g$ (where g is the acceleration of gravity). This can be explained with the aid of Fig. 8 that shows the hysteretic response of the links during the mainshock (blue lines) and during the mainshock-aftershock sequence (red color) corresponding to the artificial sequence M2M3. It can be seen that when the link in the first story (Link 1) reached the failure criterion as a consequence of the aftershock, the links in the stories above the link that failed have more participation on the energy dissipation of the structure.

It is also interesting to examine the response of the elements (beams, columns, and braces) that surrounds the link that reached the failure criterion. For this purpose, Fig. 9 illustrates the hysteretic response of the four beams and columns that belong to the same story of Link 1 as well as its supporting braces before (blue line) and after reaching the failure criterion (red line). It can be seen that the surrounding elements

behave practically in an elastic manner, which is consistent with the design philosophy for EBFs, but the beams and columns behave highly nonlinearly after the Link 1 reached the failure criterion.

The influence of taking into account the link failure criterion (FC) or neglecting the failure criterion (WFC) in the seismic response is examined under individual seismic sequences. For example, Fig. 10 shows the evolution of mean IDR as the $S_a(T_1)$ increases for the model 4N_EBF under the mainshock and the mainshock-aftershock sequence M2M6 with V_A/V_M ratio equal to 1 (Set A). From the figure, it can be seen that, in general, including or not the failure criterion under the mainshock (M) does not have significant influence on the seismic response up to high levels of seismic intensity (e.g. $S_a(T_1) = 1.9g$). This can be attributed to the fact that the links are able to dissipate the energy induced by the mainshock without reaching the failure criterion. However, the seismic response of the EBF under the mainshock-aftershock sequence (S) is significantly different when failure criterion is included in the model, since it triggers larger IDR demands for intensities of around $S_a(T_1) = 1.3g$, than the EBF that neglects a failure criterion in the links. Therefore, the inclusion of a failure criterion in the seismic response of EBFs is particularly important and it should be included when evaluating the performance of EBFs under aftershocks.

In addition, Fig. 11 illustrates the evolution of peak IDR as the

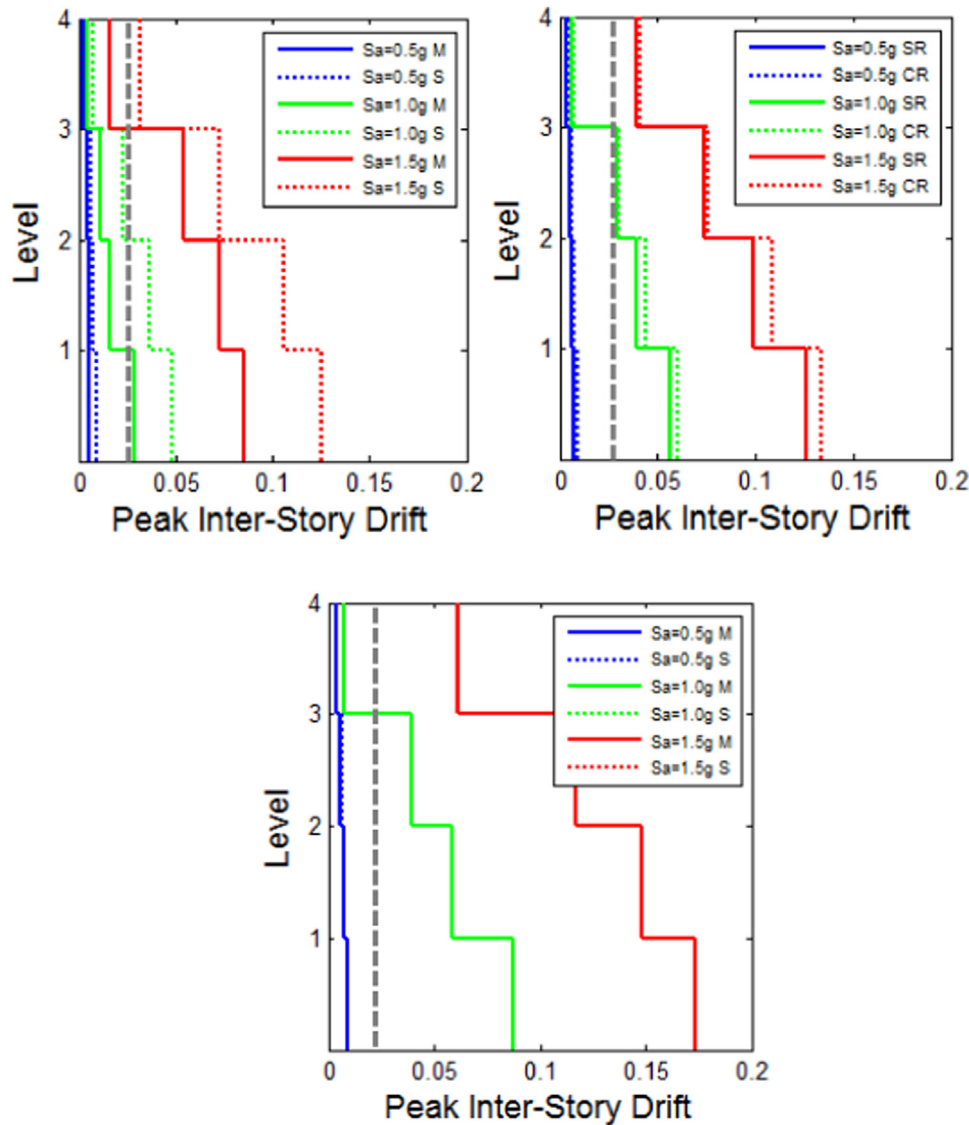


Fig. 13. Distribution of median peak inter-story drift for model 4N_EBF for three intensity levels: 0.5 g, 1.0 g, 1.5 g under three seismic sequence sets: a) $V_A/V_M = 1.0$, b) $V_A/V_M = 0.7$, and c) $V_A/V_M = 0.35$.

ground motion intensity increases of the model 8N_EBF under mainshock-aftershock sequences with $V_A/V_M = 1$. In this case, it can be observed that peak IDR exceeds the limiting IDR of 0.02 for an intensity $S_a(T_1)$ around 0.8 g, and it significantly increases for an intensity of around 1.1 g. around begin to significantly increases after an intensity of around $S_a(T_1) = 1.1$ g. Additionally, the hysteretic response of the links during the mainshock (blue lines) and during the mainshock-aftershock sequence (red color) corresponding to the artificial sequence M2R5 is shown in Fig. 12. It can be seen that the link in the third story (Link 3) has large energy dissipation under the mainshock, and it reaches the failure criterion under the aftershock. Therefore, it can be concluded that the case-study EBFs do not have a uniform hysteretic energy distribution along-height, which lead to a nonuniform distribution of damage and it constrains the efficient utilization of the energy dissipation capacity of the shear links.

4.2. Effect of ground motion intensity

To discuss the effect of the aftershocks in the nonlinear response of the case-study frames, the evolution of median peak inter-story drift demands triggered by the mainshocks (M) and the mainshock-aftershock sequences (S) corresponding to three intensity levels of each set

of earthquake ground motions described in Section 3 is shown in Fig. 13 and 14 for the 4-story and 8-story EBFs, respectively. It can be seen that median peak inter-story drift is significantly increased when the pair of mainshock-aftershock ground motions have a V_A/V_M ratio equal to one, but the increment is practically negligible when the V_A/V_M ratio decreases to 0.35. For mainshock-sequences with V_A/V_M ratios equal to one, the level of increment in peak interstory drift increases as the ground motion intensity measure, S_a , increases. It can also be observed that median peak interstory drifts tend to concentrate in the bottom story of the 4-story EBF, while they tend to concentrate in the lower stories for the 8-story EBF. The observation of peak interstory drift concentration is consistent with results from previous studies e.g. [33,34]. With reference to Figs. 8 and 12, it is also noted that the hysteretic energy distribution of the shear links is not nonuniform along-height, which led to concentration of interstory drifts at the bottom stories. This issue contributes to increase the peak interstory drift demands as a consequence of the aftershocks. Therefore, it is pertinent to investigate a design methodology that promotes uniform damage and avoids drift concentration such as those introduced in Refs. [24,35].

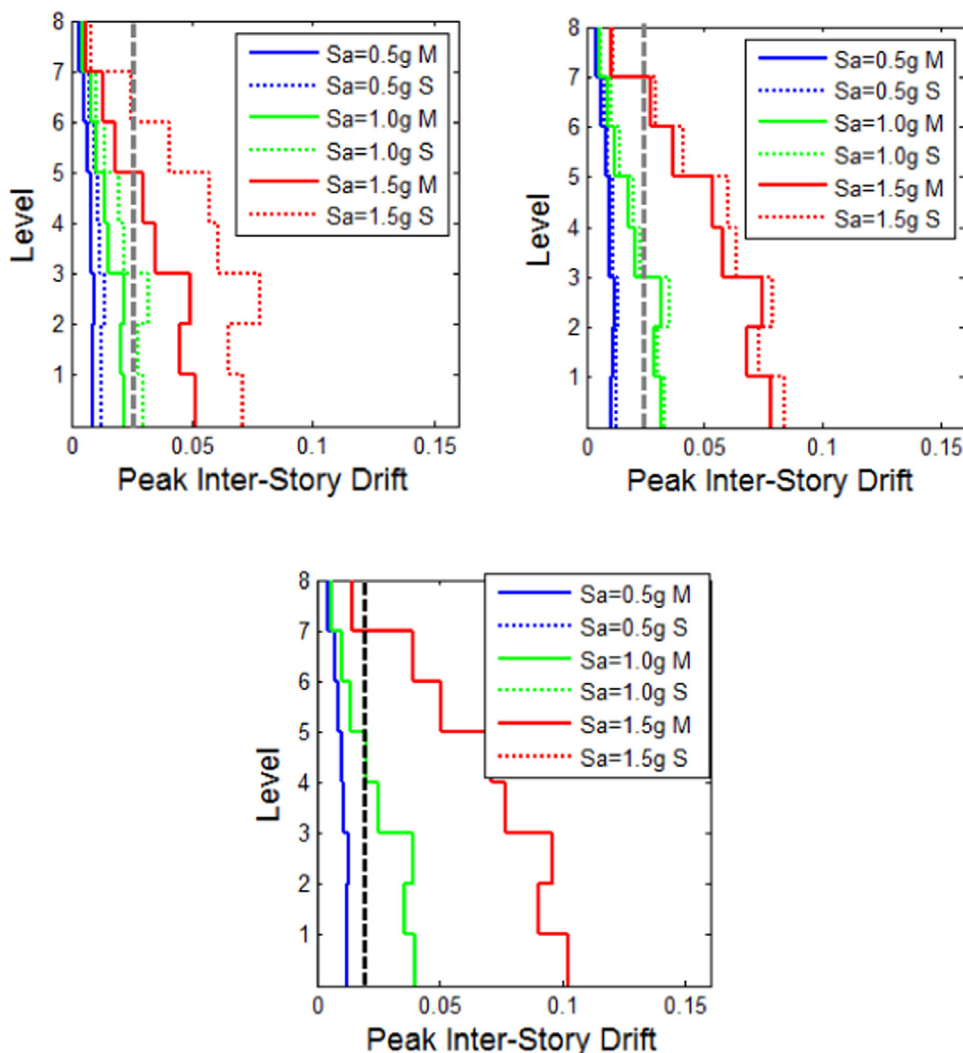


Fig. 14. Distribution of median peak inter-story drift for model 8N_EBF for three intensity levels: 0.5 g, 1.0 g, 1.5 g under three seismic sequence sets: a) $V_A/V_M = 1.0$, b) $V_A/V_M = 0.7$, and c) $V_A/V_M = 0.35$.

5. Summary and conclusions

This paper examined the seismic behavior of two steel eccentrically braced frames (EBF) assumed to be located at a soft soil site in Mexico City. The EBFs were designed to satisfy the lateral strength and stiffness requirements of the 2004 Edition of the Technical Requirements for Seismic Design prescribed in the Mexico City Building Construction Code. The analytical models of the EBFs, beams, columns, and braces were modeled using a distributed plasticity approach, while the links were modeled using a modeling strategy that simulate shear plastic hinges. In addition, the hysteretic response of the links considered a failure criterion (i.e. the links exhaust their shear capacity when an inelastic plastic rotation equal to 0.06 rad is reached during cyclic loading), which is consistent with its experimental response. Due to the scarcity of enough recorded mainshock-aftershock sequences at soft soil sites, three sets of artificial sequences with different intensity ratio, V_A/V_M (i.e. ratio of the intensity of the aftershock with respect to the mainshock, considering that the mainshocks are scaled to reach the highest PGV recorded during the September 19, 1985 earthquake in Mexico City) were generated as part of this study. The case-study EBF models were analyzed via incremental dynamic analyses, and relevant results are as follows:

- Seismic sequences with V_A/V_M ratios equal or greater than 0.7 can

significantly increase the peak inter-story drift demands in the case-study EBFs.

- Including a link failure criterion, such as that observed in experimental tests, should be included in the modeling approach of shear links while evaluating the seismic performance of the EBFs analytical models.
- Once the link reached the failure criterion (i.e. 0.06 rad), generally under the aftershocks, the beams and columns that surround the links behaved nonlinearly, which is opposite to the design philosophy for EBFs. As a consequence, peak inter-story drift demand significantly increases.
- It was noted that the hysteretic energy distribution of the shear links was nonuniform along-height, which led to concentration of inter-story drifts at the bottom stories, under earthquake ground motions typical of soft soil conditions in Mexico City.

Therefore, it can also be concluded that adequate detailing should be provided to assure that the link can develop plastic link rotations above code requirements without premature failure under seismic sequences to avoid that the surrounding elements experience nonlinear behavior. Additionally, follow-up studies should focus on providing a methodology to optimize the hysteretic energy distribution of the EBFs and to take advantage of the energy dissipating capacity of the links.

Acknowledgements

The first author would like to thank the *Universidad Michoacana de San Nicolás de Hidalgo*, while the second and third author would like to acknowledge the *Universidad Autónoma de Sinaloa* in Mexico. The authors also express their gratitude to the Consejo Nacional de Ciencia y Tecnología (CONACYT) in Mexico for funding the research reported in this paper.

References

- [1] American Institute of Steel Construction, Inc., (AISC). Seismic provisions for structural steel buildings. Standard ANSI/AISC 341-16. Chicago (IL, USA): AISC; 2016.
- [2] Azad SK, Topkaya C. A review of research on steel eccentrically braced frames. *J Constr Steel Res* 2017;128:53–73.
- [3] Kanvinde AM, Grilli DA, Marshall KA. Framework for forensic examination of earthquake-induced steel fracture based on the field failures in the 2011 Christchurch earthquake. In: Proceedings of the 15th world conference on earthquake engineering, Lisbon, Portugal; 2012.
- [4] Kanvinde AM, Marshall KS, Grilli DA, Bomba G. Forensic analysis of link fractures in eccentrically braced frames during the February 2011 Christchurch earthquake – testing and simulation. *J Struct Eng ASCE* 2014;141(5).
- [5] Gaceta Oficial de la Ciudad de México. Technical Requirements for Design of Steel Structures; 2017 (In Spanish). (<https://www.smig.org.mx/archivos/NTC2017/normas-tecnicas-complementarias-reglamento-construcciones-cdmx-2017.pdf>).
- [6] Arroyo D, Ordaz M. Hysteretic energy demands for SDOF systems subjected to narrow band earthquake ground motions. Applications to the lake bed zone of Mexico City. *J Earthq Eng* 2007;11:147–65.
- [7] Teran-Gilmore A, Jirsa JO. Energy demands for seismic design against low-cycle fatigue. *Earthq Eng Struct Dyn* 2007;36(3):383–404.
- [8] Quinde P, Reinoso E, Terán-Gilmore A. Inelastic seismic energy spectra for soft soils: application to Mexico City. *Soil Dyn Earthq Eng* 2016;89:198–207.
- [9] Rosenblueth E, Meli R. The 1985 Mexico earthquake: causes and effects in Mexico city. *Concr Int (Acids)* 1986;8:23–34.
- [10] Ruiz-García J, Marín MV, Terán-Gilmore A. Effect of seismic sequences in reinforced concrete frame buildings located in soft-soil sites. *Soil Dyn Earthq Eng* 2014;63:56–68.
- [11] Díaz-Martínez G, Ruiz-García J, Terán-Gilmore A. Response of structures to seismic sequences corresponding to Mexican soft soils. *Earthq Struct* 2014;7:1241–58.
- [12] Guerrero H, Ruiz-García J, Escobar JA, Terán-Gilmore A. Response to seismic sequences of short-period structures equipped with Buckling-Restrained Braces located on the lakebed zone of Mexico City. *J Constr Steel Res* 2017;137:37–51.
- [13] OpenSees. Open system for earthquake engineering simulation - Home Page. (<http://opensees.berkeley.edu/>) (September 1).
- [14] Gaceta Oficial del Distrito Federal. Technical Requirements for Seismic Design4. (In Spanish). (<http://www.smie.org.mx/informacion-tecnica/normas-tecnicas-complementarias.php>).
- [15] Applied Technology Council (ATC). Modeling and acceptance criteria for seismic design and analysis of tall buildings, ATC 72-1, Redwood City, CA, USA; 2010.
- [16] Krawinkler H. shear in beam shear in beam-column joints in seismic design of steel frames. *Eng J (AISC)* 1978;15:82–91.
- [17] Richards PW. Cyclic stability and capacity design of steel eccentrically braced frames, Ph.D. dissertation. San Diego, La Jolla, CA: Dept. of Structural Engineering, Univ. of California; 2004.
- [18] Prinz GS. Using buckling-restrained braces in eccentric configurations, Ph.D. Dissertation. Brigham Young University; 2010.
- [19] Ramadan T, Ghobarah A. Analytical model for shear-link behavior. *J Struct Eng ASCE* 1995;121:1574–80.
- [20] Okazaki T, Engelhardt MD. Cyclic loading behavior of EBF links constructed of ASTM A992 steel. *J Constr Steel Res* 2007;63:751–65.
- [21] Okazaki T, Engelhardt MD, Drolias A, Shell E, Honge J-K. Experimental investigation of link-to-column connections in eccentrically braced frames. *J Constr Steel Res* 2009;65:1401–12.
- [22] Gulec CK, Gibbons B, Chen A, Whittaker AS. Damage states and fragility functions for link beams in eccentrically braced frames. *J Constr Steel Res* 2011;67(9):1299–309.
- [23] Mexican Strong Motion Dataset 1960–1999. Mexican Society of Seismic Engineering, A.C. (<http://www.unam.mx/db/spanish/pubesp.html>).
- [24] Park K, Medina RA. Conceptual seismic design of regular frames based on the concept of uniform damage. *J Struct Eng* 2007;133(7):945–55.
- [25] Roeder CW, Popov EP. Inelastic behavior of eccentrically braced steel framed systems under cyclic loading. Report UCB/EERC-77/18. Berkeley: Earthquake Engineering Research Center; 1977.
- [26] Ricles JM, Popov EP. Dynamic analysis of seismically resistant eccentrically braced frames. Report UCB/EERC-87/07. Berkeley: Earthquake Engineering Research Center; 1987.
- [27] Bosco M, Marino EM, Rossi PP. Modelling of steel link beams of short, intermediate or long length. *Eng Struct* 2015;84:406–18.
- [28] Bosco M, Gherzi A, Marino EM, Rossi PP. Importance of link models in the assessment of the seismic response of multi-storey ebfs designed by ec8. *Ing Sismica* 2016;33(3):82–93.
- [29] Lee K, Foutch DA. Performance evaluation of damaged steel frame buildings subjected to seismic loads. *J Struct Eng* 2004;130(4):588–99.
- [30] Li Q, Ellingwood BR. Performance evaluation and damage assessment of steel frame buildings under main shock-aftershock sequences. *Earthq Eng Struct Dyn* 2007;36:405–27.
- [31] Miranda E. Evaluation of site-dependent inelastic seismic design spectra. *J Struct Eng ASCE* 1993;119:1319–38.
- [32] Trifunac MD, Brady AJ. A study on the duration of strong earthquake ground motion. *Bull Seismol Soc Am* 1975;65(3):581–626.
- [33] Foutch DA. Seismic behavior of eccentrically braced steel building. *J Struct Eng ASCE* 1989;115(8).
- [34] Rossi PP, Lombardo A. Influence of link overstrength factor on the seismic behavior of eccentrically braced frames. *J Constr Steel Res* 2007;63:1529–45.
- [35] Bosco M, Rossi PP. A design procedure for dual eccentrically braced frames: analytical formulation. *J Constr Steel Res* 2013;80:440–52.
- [36] Bojorquez E, Díaz M, Ruiz S, García FE. Seismic reliability of buildings (four-to-ten stories) located at soft soil sites of Mexico city designed under the 2004 Mexico city building construction code (In Spanish). *Rev De Ing Sismica* 2007;76:1–27. (<http://www.redalyc.org/pdf/618/61807602.pdf>).
- [37] Díaz A. Seismic reliability of steel buildings designed under the Mexico City Building Construction Code (In Spanish). *Engrg M. Thesis, National Autonomous University of Mexico.* (<http://132.248.52.100:8080/xmlui/bitstream/handle/132.248.52.100/892/DIAZGONZALEZ.pdf?Sequence=1>).